instance, a triaxial one. This means that backbending is caused by a sudden change of deformation [Th 73, SV 73].

(ii) The second band is not superfluid, as in the ground state band. This would interpret backbending as a phase transition from a superfluid to a normal-fluid state (Mottelson–Valatin effect [MV 60]).

(iii) The second band is a two quasi-particle band of particles which are rotationally aligned along the axis of rotation (see Sec. 3.3). Then backbending would correspond to a sudden alignment of a pair of nucleons (as proposed by Stephens and Simon [SS 72a]).

The general result of theoretical investigations, which include all these degrees of freedom (see Sec. 7.7), is that for the well deformed nuclei (the classical rotors) the reduction of the pairing correlations is only responsible for the slow change of the moment of inertia at low spin values, but that sudden effects such as backbending are due to alignment of a single high j pair of nucleons. There is also a large number of experimental indications [GSD 73, RSS 74, WBB 75, NLM 76, St 76] for this interpretation of the backbending phenomenon.

In the rare earth nuclei, the $i_{13/2}$ neutrons play an essential role. There is, however, experimental evidence for a second irregularity at spins of $\sim$ 26–30 $\hbar$ [LAD 77, BBB 79a] a so-called *second backbending*, which has been interpreted as the alignment of an $h_{11/2}$ proton pair [FP 78]. Other high j-orbitals may play similar roles in different regions of the periodic table.

3.3 The Particle-plus-Rotor Model

To describe the interplay between the motion of particles and the collective rotation, Bohr and Mottelson [BM 53] proposed to take into account only a few so-called valence particles, which move more or less independently in the deformed well of the core, and to couple them to a collective rotor which stands for the rest of the particles. The division into core and valence particles is not always unique. It is, however, reasonable to use the unpaired nucleon in an odd mass nucleus as a valence nucleon on an even–even core. One also can attribute the particle and the hole of a particle–hole excitation to the valence particles. More generally, one divides the Hamiltonian into two parts: an intrinsic part H_{intr}, which describes microscopically a valence particle or a whole subgroup of particles near the Fermi level; and a phenomenological part H_{coll} which describes the inert core:

$$H = H_{\text{intr}} + H_{\text{coll}}. \tag{3.10}$$

The *intrinsic part* has the form

$$H_{\text{intr}} = \sum_k \epsilon_k a_k^+ a_k + \frac{1}{4} \sum_{klmn} \bar{v}_{klmn} a_k^+ a_l^+ a_n a_m, \tag{3.11}$$

where ϵ_k are single-particle energies in the deformed potential (e.g., Nilsson energies) and $\bar{v}$ is the interaction between the valence particles which is, or can be, neglected in many cases.*

The *collective part* describes the rotations of the inert core:

$$H_{\text{coll}} = \frac{R_1^2}{2\vartheta_1} + \frac{R_2^2}{2\vartheta_2} + \frac{R_3^2}{2\vartheta_3}, \tag{3.12}$$

where the R_i are the body-fixed components of the collective angular momentum of the core. Together with the angular momentum of the valence particles $\mathbf{j}$ (which is the sum over the single-particle angular momenta) it forms the total angular momentum $\mathbf{I}$ (see Appendix A):

$$\mathbf{I} = \mathbf{R} + \mathbf{j}. \tag{3.13}$$

Eliminating $\mathbf{R}$, H_{coll} can be decomposed into three parts:

$$H_{\text{coll}} = H_{\text{rot}} + H_{\text{rec}} + H_{\text{cor}}, \tag{3.14}$$

where

$$H_{\text{rot}} = \frac{I_1^2}{2\vartheta_1} + \frac{I_2^2}{2\vartheta_2} + \frac{I_3^2}{2\vartheta_3} \tag{3.15}$$

is the pure rotational operator of the rotor [Eq. (1.55)], which acts only on the degrees of freedom of the rotor, that is, the Euler angles. The term

$$H_{\text{rec}} = \sum_{i=1}^{3} \frac{j_i^2}{2\vartheta_i} \tag{3.16}$$

is usually called the recoil term. It represents a recoil energy of the rotor. This operator acts in the coordinates of the valence particles only. For more than one valence particle, it contains a two-body interaction.

Finally, the coriolis interaction

$$H_{\text{cor}} = -\sum_{i=1}^{3} \frac{I_i j_i}{\vartheta_i} \tag{3.17}$$

couples the degrees of freedom of the valence particles to the degrees of freedom of the rotor. This purely kinematic coupling is the only coupling in the model.

It should be noticed that the total angular momentum operators in the laboratory system I_x, I_y, I_z commute with the Hamiltonian (3.10). Although the rotational symmetry is violated in the intrinsic frame (e.g., in the Nilsson Hamiltonian), the model conserves angular momentum for the total system, because the operators I_x, I_y and I_z act only on the Euler angles and commute with the intrinsic components I_1, I_2 and I_3 (see Appendix A). However, it must be emphasized that this rotational invariance is achieved only through the introduction of a phenomenological

*We will see in Chapter 6 that pairing correlations play an important role in deformed nuclei and we should therefore talk about quasi-particles rather than particles. This only yields simple occupation factors to the formulae shown below, which we give sometimes for the sake of completeness, however. For a deeper understanding, the reader is referred to Chapter 6.

core. If one wants to treat all particles microscopically (the limit of vanishing core), the Euler angles are redundant variables (see Sec. 11.3).

The wave function of the system may be written as

$$|\Psi_M^I\rangle = \sum_K \Phi_K |IMK\rangle, \tag{3.18}$$

where Φ_K depends on the coordinates of the valence particles and the $|IMK\rangle$ depend on the Euler angles and are defined in Eq. (A.21). In the simplest case, there is only one valence particle and an axially symmetric rotor. Using this model a large number of the experimental spectra of odd nuclei has been reproduced very accurately, and from this point of view it is certainly one of the most powerful models in nuclear physics. However, until now a clear-cut microscopic derivation has been missing. Such a derivation should start from a many-body Hamiltonian (2.19). The set of $3A$ particle coordinates should be transformed in a proper way into a set of $3A-3$ internal coordinates and 3 Euler angles which describe the collective motion. To this transformation should correspond a decomposition of the Hamiltonian into an internal and a collective part, as in Eq. (3.10). Finally, one could hope to describe the internal motion by a deformed shell model.

Many attempts have been made in this direction and we give a short discussion of them in Section 11.3, but up to the present time the problem has still not been completely solved. In the case of well deformed nuclei the model can be backed by the following arguments.

(i) Microscopic Hartree–Fock calculations show very pronounced minima in the energy surface at axial symmetric deformations, which justifies the notion of a rotating core.

(ii) The model is to some extent equivalent to the cranking model (see Sec. 3.4), which is microscopically founded at least in the limit of strong nearly axial symmetric deformations.

(iii) Villars and Cooper [VC 70] have shown that, in introducing redundant coordinates, a Hamiltonian of a form similar to that in Eq. (3.10) can be found with, however, additional coupling terms. In the limit of strong deformation and with further assumptions, they obtained the correct expression for the moment of inertia.

The particle-plus-rotor model has, however, also been applied with great success to nuclei in the region of small deformations and to transitional nuclei. It is not clear at the present time how this can be explained microscopically.

3.3.1 The Case of Axial Symmetry

Assuming that the rotor has the 3-axis as axis of symmetry, that is, $\vartheta_1 = \vartheta_2 = \vartheta$, there can be no collective rotation around this axis and the 3-component of $\mathbf{R}$ has to vanish (see Sec. 1.5). From Eq. (3.13) it follows

immediately that K, the 3-component of the total angular momentum I, has to be equal to Ω, the 3-component of j:

$$K = \Omega. \tag{3.19}$$

For the different terms of the Hamiltonian (3.10), (3.14), we obtain in this case

$$H_{\text{intr}} = \sum_{i,\Omega} \epsilon^i_\Omega a^+_{i\Omega} a_{i\Omega}, \tag{3.20}$$

$$H_{\text{rot}} = \frac{\mathbf{I}^2 - I_3^2}{2\vartheta}, \tag{3.21}$$

$$H_{\text{rec}} = \frac{1}{2\vartheta}(j_1^2 + j_2^2), \tag{3.22}$$

$$H_{\text{cor}} = -\frac{1}{\vartheta}(I_1 j_1 + I_2 j_2) = -\frac{1}{2\vartheta}(I_+ j_- + I_- j_+). \tag{3.23}$$

In (3.20) we have neglected the residual interaction. The single-particle levels in the axially symmetric well are labeled by $k = (i, \Omega)$ and the corresponding eigenfunctions will be denoted by Φ^i_Ω.

The recoil term acts only in the intrinsic coordinates. It is often neglected, because the intrinsic single-particle energies ϵ^i_Ω are adjusted to experimental data. We follow this argument in the following discussion and omit H_{rec} for the moment. Only in Section 3.3.2.1 will we take it up again. The Hamiltonian (3.20–3.23) has eigenfunctions of the type (3.18), which can be found by a numerical diagonalization of the Hamiltonian (3.10). However, the different terms in (3.20–3.23) are of different importance, depending on the physical situation. Therefore, it is useful to consider three limits in which one of the terms becomes predominant and which as a consequence can be solved analytically (for a review, see [St 75a]):

In the *strong coupling limit*, the odd particle adiabatically follows the rotations of the even mass core. It is realized if the coupling to the deformation is much stronger than the perturbation of the single particle motion by the Coriolis interaction.

In the *weak coupling limit*, which is realized for very small deformations, the odd particle essentially moves on spherical shell model levels only slightly disturbed by, for example, the quadrupole vibrations (see Sec. 9.3.3).

In the *decoupling limit*, the Coriolis force is so strong that the coupling to the deformation of the core may be neglected. The total angular momentum and the single-particle angular momentum are then parallel to one another.

3.3.1.1 The Strong Coupling Limit (Deformation Alignment). The strong coupling limit is realized when the Coriolis interaction matrix elements are small compared with the level splitting of the single-particle energies in the deformed shell model for different values of Ω. We should expect that this

is the case

(i) for large deformations β, because the level splitting in the Nilsson Hamiltonian is $\propto \beta$, whereas the rotational constant $\hbar^2/2\vartheta$ is, according to a simple empirical rule (Eq. (1.50), $\propto \beta^{-2}$; and

(ii) for small Coriolis matrix-elements. As we shall see in Eq. (3.33), they are $\propto [(I(I+1)-K^2)(j(j+1)-\Omega^2)]^{1/2}$, that is, they are small either for low spins I or for nucleons in orbitals with small particle angular momenta j. For large j-values they can only be neglected for high Ω values.

It is called the *strong coupling* or *deformation aligned* limit because in this case K is a good quantum number. The angular momentum $\mathbf{j}$ of the valence particles is strongly coupled to the motion of the core. In a semiclassical picture, $\mathbf{j}$ precesses around the 3-axis, which is shown in the coupling scheme of Fig. 3.7a. Since H_{cor} is the only term in the Hamiltonian which couples the particle and rotor degrees of freedom, the eigenfunctions are in this limit products of the functions Φ^j_K (eigenfunctions of H_{intr}, e.g., the single-particle Nilsson functions) and the eigenfunctions of the symmetric rotor $|IMK\rangle$ (see Appendix A).

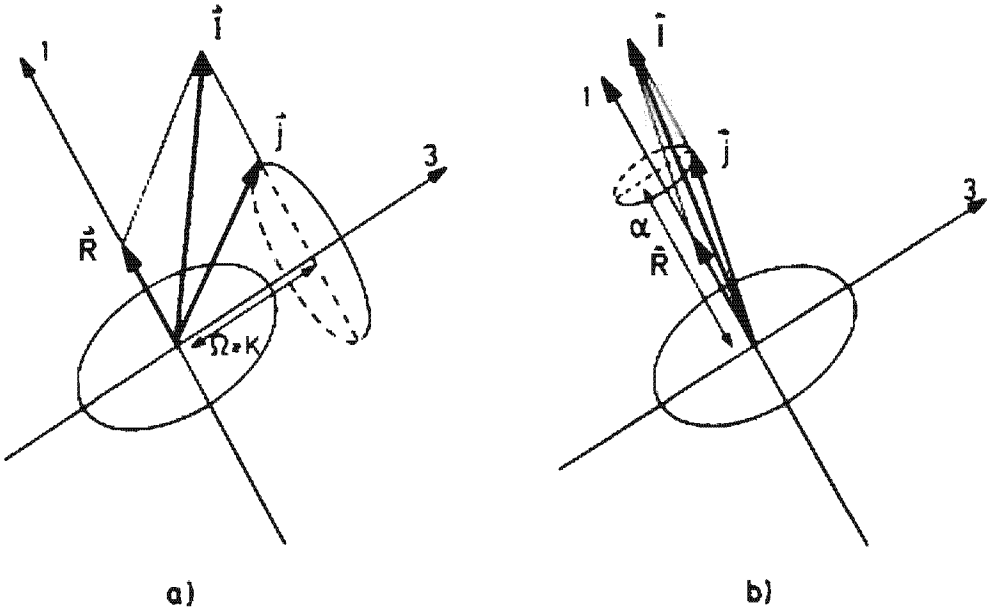

Figure 3.7. Coupling schemes in the particule-plus-rotor model: (a) strong coupling; (b) rotational alignment.

We have seen in Section 1.5.1 that the Hamiltonian (3.10) has an additional symmetry, $\mathcal{R}_1$, which describes a rotation of the core by 180° around the 1-axis of the body-fixed system

$$\mathcal{R}_1 = e^{i\pi R_1} = e^{i\pi I_1} e^{-i\pi j_1}. \tag{3.24}$$

We therefore have to symmetrize the wave function (3.18) and get together with Eq. (A.24) the following set of eigenfunctions [Ke 56]

$$|\Psi^I_{MK}\rangle \frac{1}{\sqrt{2(1+\delta_{K0})}} \{\Phi^j_K |IMK\rangle + (-)^I e^{-i\pi j_1} \Phi^j_K |IM-K\rangle\}. \tag{3.25}$$

If we know the decomposition of Φ^i_K into eigenstates of $\mathbf{j}^2$

$$|\Phi^i_{K=\Omega}\rangle = \sum_{nj} C^i_{nj}|nj\Omega\rangle, \tag{3.26}$$

we find

$$e^{-i\pi j_1}|\Phi^i_{K=\Omega}\rangle = \sum_{nj} C^i_{nj}(-)^{-j}|nj-\Omega\rangle. \tag{3.27}$$

The energy spectrum which corresponds to (3.25) is given by

$$E^i_K(I) = \epsilon^i_K + \frac{1}{2\mathfrak{I}}\left(I\cdot(I+1)-K^2\right) \tag{3.28}$$

[usually, instead of ϵ^i_K in (3.28), we have quasi-particle energies E^i_K as they are defined in Eq. (6.72)]. This is the spectrum of a rotational band. The lowest possible spin is $I_0 = K$. The bandhead $E^i_K(I_0)$ is not precisely ϵ^i_K, but shifted a little, especially if we take into account the recoil term and the residual interaction. The spectrum has a spacing $\Delta I = 1$ and its moment of inertia is that of the rotor.

In this strong coupling limit we have neglected the Coriolis interaction completely. Taking it into account at least in first order perturbation theory, we get a contribution only for $K = 1/2$ bands

$$E^i_{K=1/2}(I) = \epsilon^i_{K=1/2} + \frac{1}{2\mathfrak{I}}\left\{I(I+1) - \frac{1}{4} + a^i\left(I+\frac{1}{2}\right)(-)^{I+1/2}\right\}, \tag{3.29}$$

where the so-called *decoupling factor* is given by

$$a^i = i\langle\Phi^i_{1/2}|j_+ e^{-i\pi j_1}|\Phi^i_{1/2}\rangle \tag{3.30}$$

or if Φ^i_K is of the form (3.26),

$$a^i = -\sum_{nj}|C^i_{nj}|^2(-)^{j+1/2}(j+\tfrac{1}{2}). \tag{3.31}$$

This means, for example, that for a positive decoupling factor (major components with $j+\frac{1}{2}$ odd) the levels with odd values of $I+\frac{1}{2}$ ($I = \frac{1}{2}, \frac{5}{2}, \frac{7}{2}, \cdots$) are shifted downwards. This explains very nicely the rather distorted bands for $K = \frac{1}{2}$ in many nuclei [ABH 56] where there are, in fact, two bands having $\Delta I = 2$ each (even and odd values of $I+\frac{1}{2}$) shifted against one another. The reason for this decoupling comes from the symmetrization Eq. (3.25) with respect to $\mathfrak{R}_1$ mixing states with $K = \frac{1}{2}$ and $K = -\frac{1}{2}$ via the Coriolis matrix elements. The strength of the decoupling factor a^i depends on the j-components which contribute to the single-particle wave function $\Phi^i_{1/2}$. If levels with large single-particle angular momenta are involved, it is very strong. However, perturbation theory is no longer valid in such cases, and also other matrix elements of the Coriolis operator come into play. Therefore, the strong coupling limit is no longer realized and we have to consider a different limit.

3.3.1.2 The Weak Coupling Limit (No Alignment). As we have said, the strong coupling approximation breaks down if the Coriolis matrix elements are no longer negligible compared to the energy splitting of the single-

particle levels belonging to different K values. Let us therefore study the Coriolis matrix elements in more detail.

$$\langle \Psi'_{MK+1}|H_{\text{cor}}|\Psi'_{MK}\rangle = -\frac{1}{\mathfrak{J}}\sqrt{I(I+1)-K(K+1)}\ \langle \Phi_{\Omega+1}|j_+|\Phi_\Omega\rangle. \quad (3.32)$$

If Φ_Ω is of the form shown in Eq. (3.26), we obtain

$$\langle \Psi'_{MK+1}|H_{\text{cor}}|\Psi'_{MK}\rangle = -\frac{1}{2\mathfrak{J}}\sum_{nj}|C_{nj}|^2\sqrt{I(I+1)-K(K+1)}\ \sqrt{j(j+1)-\Omega(\Omega+1)}\ . \quad (3.33)$$

We see that these matrix elements are large for large values of I/K and j/Ω. That is, if, for example, levels with large j and small Ω values are involved. Particles in such levels have high angular momentum and a density distribution close to the 3-axis. Therefore, it is clear that a rotation of the core perpendicular to this axis has a great influence on the motion of these particles.

A well known example is the neutron $1i_{13/2}$ level, which lies in the vincinity of the Fermi level for light rare earth nuclei such as Dy and Er. One can estimate the Coriolis matrix element for the $\Omega=\frac{1}{2}$ case to be $0.1\times I$ [MeV], which is in fact quite large compared with the level spacing of H_{intr}. Since such levels with high j-values are drastically shifted downwards by the spin orbit term of the shell model (see Sec. 2.4) into a shell with a different N-quantum number, these levels are rather pure configurations, that is, $C_{nj}\simeq 1$ (intruder state). It is therefore sufficient in the following to consider *only one such single j-shell*. The $1i_{13/2}$ shell is not the only such case. The energy of the largest j-value in each major shell is lowered drastically and has an important role in many rotational spectra.

Vogel [Vo 70] proposed a limit (usually called weak coupling or no alignment limit) in which the K-splitting of H_{intr} is totally neglected. (This, of course, can only be a valid approximation for small deformation.) Now $\mathbf{J}^2$ and $\mathbf{R}^2$ commute with H_{intr} and we can construct eigenfunctions of $\mathbf{R}^2$ and R_3 (the eigenvalue of the latter is, of course, zero). A proper angular momentum coupling gives*

$$|\Psi^{IR}_M\rangle = \sum_K (-)^{j-K} C^{I}_{K\ -K\ 0}\Phi_K|IMK\rangle. \quad (3.34)$$

These wave functions diagonalize $\mathbf{R}^2$, and the corresponding spectrum is of the form

$$E(I) = E_{\text{intr}} + \frac{1}{2\mathfrak{J}}R(R+1), \quad (3.35)$$

with

$$|j-R| \leq I \leq j+R;\ R=0,2,4,\cdots (\mathfrak{R}_1 \text{ symmetry}). \quad (3.36)$$

This means that for each rotational quantum number R, $\mathbf{J}$ can have $2j+1$ orientations without changing the energy of the system (zero cou-

*Since we couple the angular momenta $\mathbf{I}$ and $-\mathbf{j}$ to $\mathbf{R}=\mathbf{I}-\mathbf{j}$, we have to apply a coupling rule as in the *ph*-case of Eq. (2.46).

pling). The splitting of the $2j+1$ levels can be taken into account in first-order perturbation theory (we will take a Nilsson term $\sim\beta r^2 Y_{20}$ as perturbation).

$$E(I) = E_0 + \frac{1}{2\vartheta} R(R+1) - \beta\hbar\omega_0 \langle \Psi_M^{IR} | r^2 Y_{20} | \Psi_M^{IR} \rangle. \tag{3.37}$$

To each orientation of $\mathbf{j}$ there is a whole rotational band of the core with $\Delta R = 2$. The levels with the highest I values $I = R + j$ for a given energy (i.e., for a given R) correspond to the yrast levels. These levels are connected by strong $E2$ transitions [Re 75a] and are experimentally the most easily accessible. They are called *favored states** [St 75a] and their energy is given by

$$E(I) = E_{\text{intr}} + \frac{1}{2\vartheta}(I-j)(I-j+1). \tag{3.38}$$

This means that these states lie on a parabola with a minimum at $I \simeq j$, which is experimentally widely confirmed, an example of which is shown in Fig. 3.8.

* Levels with a lesser degree of alignment (e.g. $I = j + R - 1$) are called *unfavored states*.

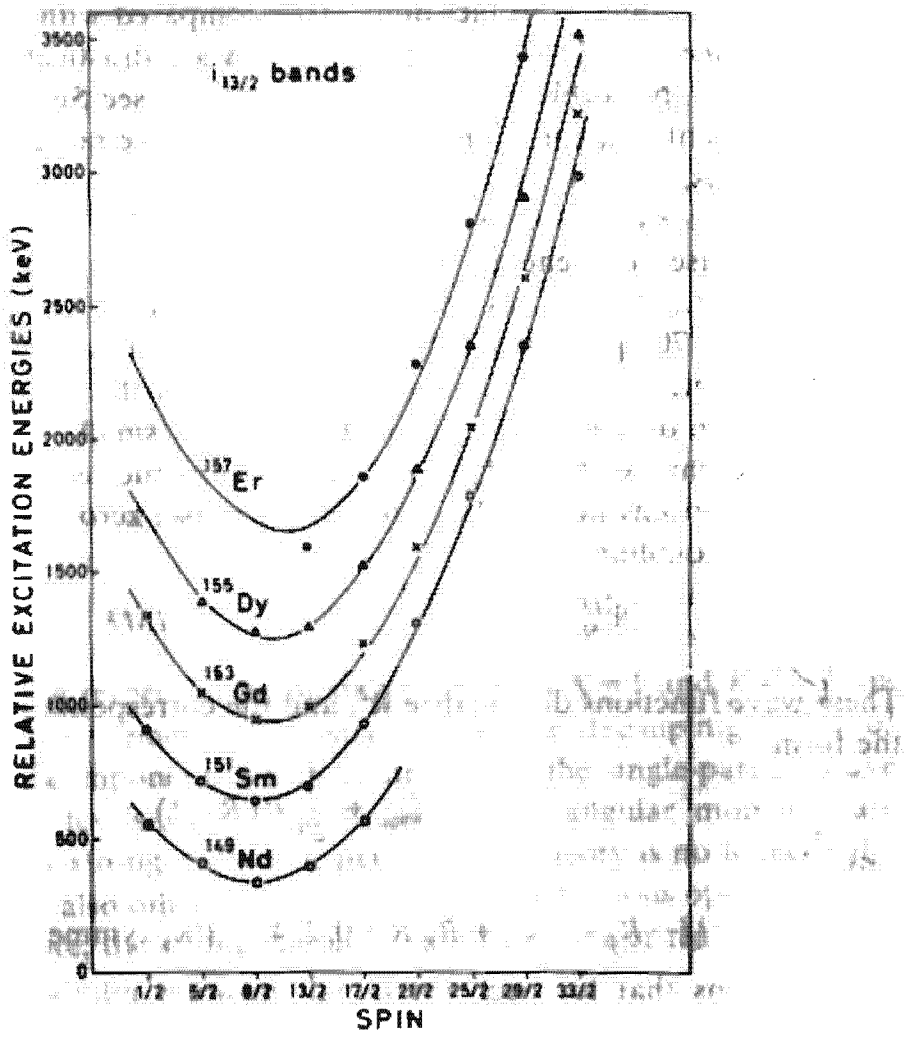

Figure 3.8. Relative excitation energies as a function of spin for the $i_{13/2}$ bands in some $N = 89$ nuclei. (The experimentally observed band members are plotted such that the $13/2^+$ states are equally spaced (300 keV).) (From [LR 76].)

On the right branch of this parabola **j** and **R** are aligned (**J** ∥ **R**),

$$I = j + R = j, j+2, j+4, \ldots,$$

and on the left branch **j** and **R** are anti-aligned (**J** ∥ $-$**R**); the core rotates in the opposite direction as **j***:

$$I = j - R = j-2, j-4, \ldots, \tfrac{1}{2} \text{ (or } \tfrac{1}{2}).$$

As an empirical rule one can say that the weak coupling limit is strictly valid only for very small deformations $|\beta A^{2/3}| < 4$. We shall see in the next section, however, that the states with **I** ∥ **j** are energetically favoured even in the case of stronger deformations, where neglecting the Ω-dependence of H_{intr} is no longer justified. Therefore, the formula (3.38) is also valid for many levels in more deformed nuclei (see for instance Fig. 3.8) in the so-called rotation aligned coupling scheme.

3.3.1.3 The Decoupling Limit (Rotational Alignment). In the case of intermediate deformations, the energy splitting in the intrinsic part of the Hamiltonian can no longer be neglected. In this case, the orientation of the external large j-particle is no longer independent of the motion of the core. Stephens et al. [SDN 73] realized that the requirement of maximal overlap of the single-particle density distribution (which is concentrated mostly in a plane perpendicular to j) with the core can be fulfilled if the external particle is aligned along the rotational axis of a prolate nucleus (see also Sec. 2.8.4).

Mathematically, we can understand this in the model of a single j-shell ($C_{nj} \simeq 1$, like, for example, in the $i_{13/2}$ case). Neglecting $\mathbf{l}^2$ and $\mathbf{ls}$-term, the Nilsson energies are simply given by the diagonal matrix element

$$\begin{aligned} \epsilon_\Omega &= \epsilon_0 - \beta \cdot \hbar\omega_0 \langle nlj\Omega | r^2 Y_{20} | nlj\Omega \rangle \\ &= \epsilon_0 + \beta k \frac{3\Omega^2 - j(j+1)}{4j(j+1)} = \epsilon_0 - \frac{1}{4}\beta k + C\Omega^2, \end{aligned} \tag{3.39}$$

where k and C do not depend on Ω. Also, the recoil term (3.22) can be calculated as a diagonal matrix element and yields

$$H_{rec} = \frac{1}{2\mathcal{I}} \{ j(j+1) - \Omega^2 \}. \tag{3.40}$$

Therefore, the Hamiltonian (3.10) in this approximation is:

$$H = \epsilon_0 - \frac{1}{4}\beta k + \frac{1}{2\mathcal{I}}(I(I+1) + j(j+1)) + \left(C - \frac{1}{\mathcal{I}}\right) I_3^2 + H_{cor}. \tag{3.41}$$

In a certain region of deformation, where $C \simeq 1/\mathcal{I}$, there is thus a cancellation of the K dependence coming from the intrinsic and rotational parts of the Hamiltonian. This turns out to apply for a rather broad domain of intermediate deformations. Unfortunately, the eigenfunctions of H_{cor} which we needed to solve (3.41) cannot be given analytically in the general case. Thus, we wish to give a qualitative discussion. Writing the

* In principle, there are also anti-aligned states with $R > j$ [PO 78].

Coriolis term in the form*

$$H_{\mathrm{cor}} = -\frac{1}{\vartheta}\mathbf{I}_{\perp}\mathbf{j}_{\perp}, \tag{3.42}$$

we see that it has its lowest expectation value for the wave functions with $\langle\mathbf{I}\rangle \parallel \langle\mathbf{j}\rangle$. Since $\mathbf{R}$ is perpendicular to the 3-axis, one gets the lowest eigenvalue for wave functions with a single-particle angular momentum aligned along a rotational axis perpendicular to the symmetry axis. For this purpose, we choose the 1-axis and accordingly construct eigenfunctions $|\tilde{\Phi}_{\alpha}\rangle$ of j_1 with eigenvalues α by rotating the eigenfunctions $|\Phi^{j}_{K}\rangle$ of j_3 through 90° about the 2-axis:

$$|\tilde{\Phi}_{\alpha}\rangle = \sum_{K} d^{j}_{K\alpha}\left(-\frac{\pi}{2}\right)|\Phi^{j}_{K}\rangle, \tag{3.43}$$

where $d^{j}_{K\alpha}$ is the Wigner function of this rotation [Ed 57].

For the total wave function it is, however, not so easy to make such a construction in which α is a good quantum number. The ansatz

$$|\Psi^{I}_{M\,j_{\alpha}}\rangle = \sum_{K} d^{j}_{K\alpha}\left(-\frac{\pi}{2}\right)\Phi^{j}_{K}|IMK\rangle \tag{3.44}$$

is an eigenfunction of H_{cor} at least for $I \gg K$. With

$$I_{-}|IMK\rangle = \sqrt{I(I+1)-K(K+1)}\;|IMK+1\rangle \simeq I|IMK+1\rangle \tag{3.45}$$

we then easily get

$$H_{\mathrm{cor}}|\Psi^{I}_{M\,j_{\alpha}}\rangle = -\frac{1}{\vartheta}I\cdot\alpha|\Psi^{I}_{M\,j_{\alpha}}\rangle \qquad (I \gg K), \tag{3.46}$$

which shows that α is the projection of $\mathbf{j}$ onto $\mathbf{I}$.

From Eq. (A24) and [Ed 57, Eq. (4.2.4)] we obtain

$$\mathcal{R}_1|\Psi^{I}_{M\,j_{\alpha}}\rangle = (-)^{I-\alpha}|\Psi^{I}_{M\,j_{\alpha}}\rangle, \tag{3.47}$$

which means that $I-\alpha$ has to be even in order to fulfill the symmetry condition $\mathcal{R}_1 = 1$.

In the case of $C \simeq 1/\vartheta$, we find for the spectrum of the Hamiltonian (3.41):

$$E(I,\alpha) = \text{const.} + \frac{1}{2\vartheta}(I(I+1)+j(j+1)-2I\alpha)$$

$$= \text{const.} + \frac{1}{2\vartheta}(I-\alpha)(I-\alpha+1) \tag{3.48}$$

$$= \text{const.} + \frac{1}{2\vartheta}R(R+1) \tag{3.49}$$

where $R = I-\alpha = 0, 2, 4, \ldots$ has to be even because of the symmetry condition (3.47).

The lowest lying states are therefore the ones which are maximally aligned ($\alpha = j$, *favored states*). This corresponds exactly to the picture of a valence particle whose spin is oriented perpendicular to the 3-axis while

* $\mathbf{I}_{\perp}$ and $\mathbf{j}_{\perp}$ are the components of $\mathbf{I}$ and $\mathbf{j}$ perpendicular to the symmetry axis.

the core is completely decoupled and rotates with $R = I - \alpha$, giving rise to a spectrum $\Delta I = 2$, but which is otherwise equivalent to that of the neighboring even nucleus. Such bands have been seen, for example, in weakly deformed nuclei (see Figs. 3.8 and 3.9).

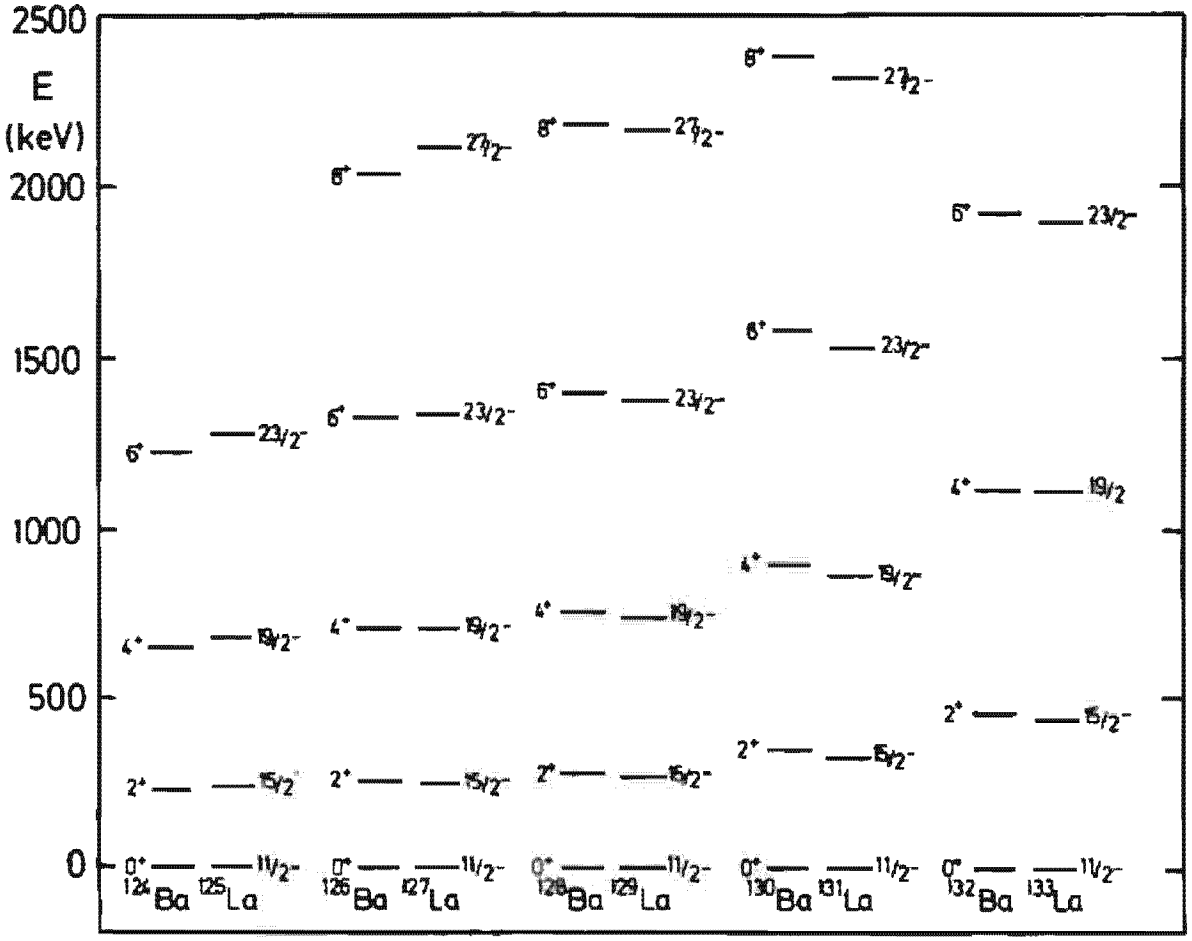

Figure 3.9. Comparison of ground band levels in some Ba isotopes with negative parity bands in the neighboring La nuclei. In most cases the La 11/2 level is not the ground state, and its energy has been subtracted from all levels shown for that isotope. (From [SDL 72].)

Lesser aligned states (*unfavored states*) have $\alpha = j - 1$. They often lie at higher energies and are then not populated in (HI, xn) reactions.

Figure 3.10 shows the exact solution of the axially symmetric particle-plus-rotor model for one valence nucleon in a $1h_{11/2}$ shell as a function of the deformation β. For very small β-values, one has the weak coupling scheme of several nearly degenerate multiplets. On the oblate side ($\beta < 0$) the strong coupling is realized. In this case, the lowest level in the Nilsson scheme (see Fig. 2.21.) is the $\Omega = 11/2$ level. Its Coriolis matrix element is very small and a strongly coupled band with $\Delta I = 1$ is observed. On the prolate side the opposite is true: The lowest level has $\Omega = \frac{1}{2}$ and a very large Coriolis matrix element. The yrast band (the levels with the highest I-values) is now formed by a decoupled band $I = 11/2, 15/2, 19/2, \ldots$ with $\Delta I = 2$ and a level spacing, which is more or less that of the rotor (as seen at $\beta = 0$). We see also that for these completely aligned yrast levels the rotation aligned coupling scheme is very well realized over a wide range of

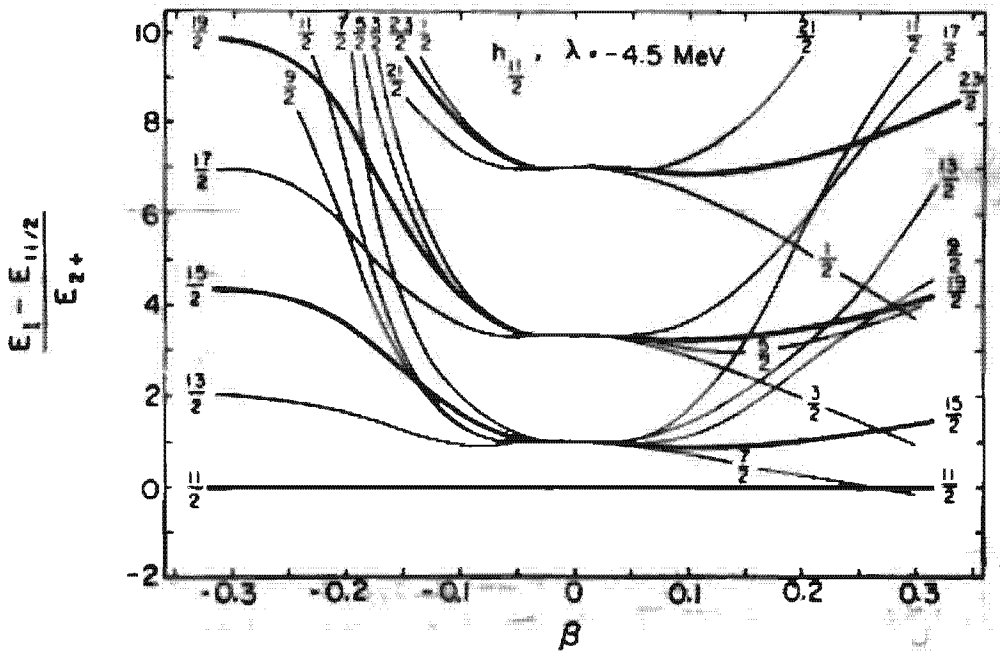

Figure 3.10. The eigenvalues of an axially symmetric particle-plus-rotor model, with one particle sitting in the $1h_{11/2}$ shell, as a function of the deformation β. Plotted are the excitation energies over the $I = 11/2$ level. The Fermi surface λ is below the entire $h_{11/2}$ orbital. (From [St 75a].)

intermediate β-values: $0.13 \sim \beta < 0.23$. Only at very large deformations does one find deviations.

The structure of the bands also depends, of course, on the position of the Fermi level. We had here the simplest case of only one particle in the shell. The complete analogue is one hole in the high j-shell. There the situation is reversed: On the prolate side are the levels with large Ω-values —that is, one observes a strongly coupled scheme—and on the oblate side are the levels with small Ω-values and a decoupled scheme.

These considerations show that the structure of the rotational bands built on such high j levels provides an excellent tool to distinguish experimentally between prolate and oblate deformations in the transition region.

Summarizing the results of this section, we can say that

(i) In many cases, the Coriolis interaction can be neglected. Then the valence nucleons rotate around the symmetry axis of the core and change their orientation with it (strong coupling $\Delta I = 1$).

(ii) In cases of small deformation and strong Coriolis interaction, the valence nucleons orient their angular momentum more or less independently of the orientation of the core. The core rotates with $\Delta I = 2$ (weak coupling).

(iii) For intermediate deformations it can happen by a cancellation effect that a rotational alignment takes place. The valence particles orient their angular momentum parallel to the collective angular momentum (perpendicular to the symmetry axis of the core) and again we have $\Delta I = 2$.

3.3.2 Some Applications of the Particle-plus-Rotor Model

The model of a few valence particles coupled to a symmetric rotor has been used in a very large number of cases to fit the experimental rotational bands. In general, it has been very successful. We do not want here to go into the many different versions which have been used but wish to discuss a few characteristic examples.

3.3.2.1 Strongly Mixed Bands in Well-Deformed Odd Mass Nuclei. The spectra of odd mass nuclei in the deformed region show many rotational bands which reveal very nicely the strong coupling picture. Only in cases where the particle sits in a single-particle shell with a high j-value (e.g., the $1i_{13/2}$ shell in the Er region), one also observes very distorted bands.* For small I values they start out like strongly coupled bands with $\Delta I = 1$, but soon we observe staggering: The levels with $I + 1/2$ even are shifted more and more against the levels with $I + 1/2$ odd, so that in the end we have two separate bands with $\Delta I = 2$ (see the positive parity band in Fig. 3.11 and [BDL 75]).

*For a comparison of these distorted bands with the backbending behavior in neighboring even nuclei, see [SKS 74].

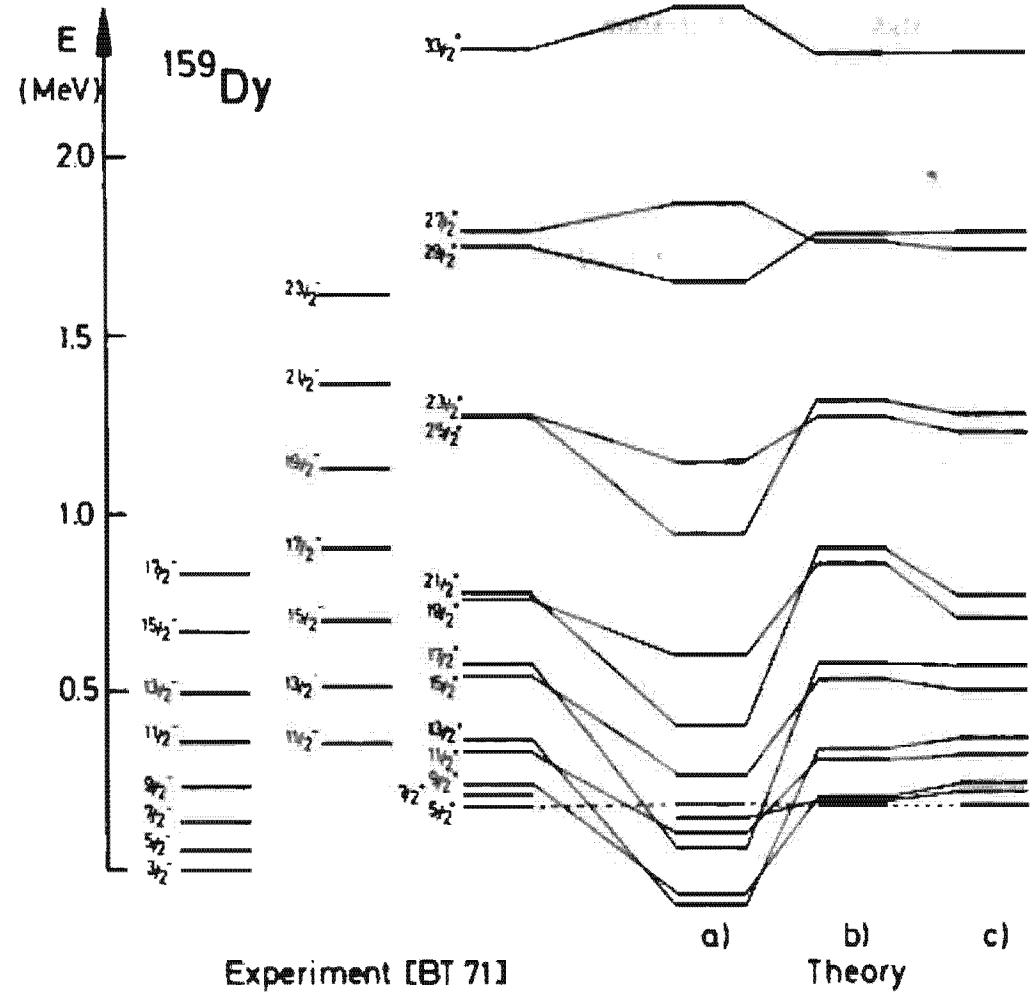

Figure 3.11. Three rotational bands in the nucleus ^{159}Dy. The $3/2^-$ and the $11/2^-$ bands are strongly coupled ($\Delta I = 1$). The positive parity band with the band head $I = 5/2$ is strongly perturbed, as discussed in the text. It is compared with three calculations: (a) a particle-plus-rotor fit without attenuation ρ, (b) a particle-plus-rotor fit with attenuation $\rho = 0.5$, and (c) a self-consistently determined attenuation according to Eq. (3.56). (From [Ri 77].)

To describe these bands one usually diagonalizes the Hamiltonian (3.10) in the strong coupling basis (3.25). The single (quasi-) particle energies are taken from a Nilsson model and the parameters like the deformation β (and the gap Δ, see Chap. 6) are used to fit the spectrum. It thereby turns out that one can only reproduce the experimental spectrum if one introduces an additional parameter ρ—the *attenuation factor*—which weakens the Coriolis interactions, that is, if we use $\rho \cdot H_{cor}$ instead of H_{cor} [HRH 70, LRB 72, HK 77]. The original Coriolis force turns out to be much too strong and it has to be reduced by a factor $\rho \sim 0.4-0.8$. With this ad hoc attenuation and the other parameters of the model reasonably chosen, we are able to reproduce the distorted bands and find that for low I-values, that is, for small Coriolis interaction, one is in the strong coupling limit with $\Delta I = 1$. For higher I-values, however, the Coriolis force gets stronger and aligns the odd particle with the large j-value parallel to the rotational axis. For I-values $I \gtrsim j$, we have a rotational aligned motion, that is, large K-mixing and a splitting of the band in favored states with maximal alignment $\alpha = j$ for $(I-j)$ even, and unfavored states with lesser alignment $\alpha = j-1$ for $(I-j)$ odd. For the same value of angular momentum R of the core, which is given by $R = I - \alpha$, these two bands are almost degenerate (see Fig. 3.11).

Several attempts have been made to explain the *attenuation factors* as a kind of effective charge in the linear response approach [BPC 72, HK 75]. It turns out that this problem is closely connected with a proper treatment of the recoil term (3.22). The argument, that it is already taken into account in the fit of the band head energies, does not apply because in the one-particle case it is proportional to $j^2 - K^2$ and therefore has a strong K-dependence which shifts the band heads [ORG 75].

To understand qualitatively the effect of the recoil term we restrict ourselves to the case of only one particle and rewrite the particle-plus-rotor Hamiltonian (3.20ff) in the following way [Kr 79].

$$H = H_{intr} + \frac{1}{2\mathcal{I}}(I(I+1) - \mathbf{j}^2) + H'_{cor} \tag{3.50}$$

with the new Coriolis term

$$H'_{cor} = -\frac{1}{\mathcal{I}}(\mathbf{I}-\mathbf{j})\mathbf{j}_\perp = -\frac{1}{\mathcal{I}}\mathbf{R}\mathbf{j} = -\omega \mathbf{j}, \tag{3.51}$$

where the collective angular velocity is given by

$$\omega = -\mathbf{R}/\mathcal{I}. \tag{3.52}$$

The Coriolis term H'_{cor} in Eq. (3.51) is attenuated compared to H_{cor} (3.23). To see this we go into the limit, where the odd particle is nearly aligned to the collective rotation $\mathbf{R}$. We then have

$$\mathbf{R} \simeq \mathbf{I}_\perp \left(1 - \frac{\alpha}{I}\right) \tag{3.53}$$

and find that H'_{cor} is in this case proportional to H_{cor}:

$$H'_{cor} = \left(1 - \frac{\alpha}{I}\right) H_{cor} = \rho \cdot H_{cor} \tag{3.54}$$

with an I-dependent attenuation factor

$$\rho = 1 - \frac{\alpha}{I}. \tag{3.55}$$

Only for very high I-values does the attenuation disappear.

So far, the discussion of the influence of the recoil term has been restricted to the pure single-particle part of this operator. In fact, it also contains a two-body

term $j_{ik} \cdot j_{lm} a_i^+ a_j^+ a_m a_k$, which produces an interaction with the particles of the core. We can treat it in the mean field approximation [Ri 77] and end up with a self-consistent attenuation factor

$$\rho = 1 - \frac{\langle j_1 \rangle}{\sqrt{I(I+1) - \langle j_3^2 \rangle}} . \tag{3.56}$$

At the limit of alignment it goes over into the form (3.55). We can also show that this approximation is equivalent to the cranking model (see Sec. 3.4). In a microscopic treatment of rotational bands in odd mass nuclei within the self-consistent cranking model (see Sec. 7.7), the attenuation of the Coriolis interaction is automatically incorporated [RMB 74, RM 74].

3.3.2.2 Backbending in Even Nuclei. The backbending phenomenon (see Sec. 3.2.4.) has been explained by Stephens and Simon [SS 72a] as an alignment of two neutrons in the $1i_{13/2}$ shell. If these two neutrons, instead of rotating around the 3-axis, align along the rotation axis of the nucleus, this adds an additional $13/2 + 11/2 = 12$ units of angular momentum. Therefore, the nucleus can decrease its collective rotation while increasing its total angular momentum through the addition of single-particle angular momentum.

To describe this idea mathematically, Stephens and Simon diagonalized the Hamiltonian (3.10) (with attenuation of the Coriolis term) taking as the basis the Slater determinant of the unperturbed core

$$|\Phi_0\rangle = |IMK = 0\rangle$$

and two quasi-particle excitations (see Chap. 7)

$$|\Phi_K\rangle = \beta_{K_1}^+ \beta_{K_2}^+ |IMK = K_1 + K_2\rangle, \tag{3.57}$$

where β_K^+ is a creation operator for a quasi-particle in the state $\Omega = K$ of the $1i_{13/2}$ shell.

For low I values, the yrast states are given mainly in the zero quasi-particle state $|\Phi_0\rangle$ of the pure rotor. The excited bands are two quasi-particle bands. For higher I-values, the particles align their angular momenta along the axis of rotation, one of them to $\alpha = j = 13/2$, the second to $\alpha = j - 1 = 11/2$. Thus, we find a mixing of the states Φ_0 and Φ_K ($K = 0, 1, \ldots$) and arrive, at the limit of full alignment, at a two-quasi-particle state of the form [see Eq. (3.44)]:

$$|\Phi\rangle_{al} = \sum_{K_1 K_2} d^j_{K_1 j}\left(-\frac{\pi}{2}\right) d^j_{K_2 j-1}\left(-\frac{\pi}{2}\right) \beta_{K_1}^+ \beta_{K_2}^+ |IMK_1 + K_2\rangle. \tag{3.58}$$

It can be written schematically as $\tilde{\beta}_j^+ \cdot \tilde{\beta}_{j-1}^+ |\Phi_0\rangle$, where the $\tilde{\beta}_\alpha^+$ are the quasi-particle operators quantized along the 1-axis.

Stephens and Simon [SS 72a] were able to reproduce the experimental backbending spectra reasonably well with this method. Since they did not take into account, however, the gradual change in the pairing correlations caused by the Coriolis–anti-pairing effect, they could not obtain the deviations from the $I \cdot (I+1)$ law at low spin values.

In spite of the fact that this model describes the important effect of two aligning particles properly, it does not allow us to decide whether there is any other mechanism which could be the origin of the observed backbending phenomenon. To decide whether it is caused by a change in shape, by a phase transition to a normal fluid state, or by an alignment process, one has to carry out a microscopic calculation which allows for all these degrees of freedom. Such investigations have been done (see Sec. 7.7). They show that the rotational alignment of two particles is

the most important effect. These processes are found in all nuclei in which a high j-shell exists in the vicinity of the Fermi surface. However, it is another question as to whether they produce backbending. This depends finally on the strength of the interaction between the two crossing bands: Only for rather small coupling matrix elements do we observe a sudden transition, that is backbending.*

3.3.3 The Triaxial Particle-plus-Rotor Model

We have already seen in Section 1.5.3 that Davydov et. al. [DF 58] used a triaxial rotor to explain the low lying 2^+ states in some transitional nuclei. The model can also be extended to odd mass nuclei by the coupling of an external particle to a triaxial rotor [Pa 61, HS 62, PR 62, PS 65, MSD 74, Me 75, FT 75, TF 75, Le 76, DF 77, LLR 78]. It has been applied to cases where the external particle sits in a high j-shell, and has turned out to be very powerful as a description of energy levels and decay schemes of many transitional nuclei.† However, at present the microscopic foundation is missing. Using microscopic theories, the calculations of static energy surfaces in these mass regions show no pronounced minima at triaxial deformations, which would justify this simple picture. In fact, there exist other models based on a *vibrational picture* [AP 76, PVD 77, YNN 76] that are also able to reproduce such spectra. It is not clear at present whether there is any connection between these two pictures of transitional nuclei.

We restrict ourselves in the following discussion to one external particle in a high j-shell (e.g., h 11/2) and couple it to a triaxial rotor. In this case, the Hamiltonian has the form [MSD 74]:

$$h = \sum_{i=1}^{3} \frac{R_i^2}{2\mathcal{I}_i} + h_0 + kr^2\beta \left\{ \cos\gamma\, Y_{20} + \sin\gamma \frac{1}{\sqrt{2}} (Y_{22} + Y_{2-2}) \right\}. \tag{3.59}$$

The β, γ-dependence of the moment of inertia $\mathcal{I}_i$ is that for irrotational flow [eq. (1.48)] and only the overall constant is adjusted. The constant k is given by the splitting of the j-shell in the Nilsson scheme. h_0 is the spherical harmonic oscillator. Usually a single-particle pairing field with constant gap Δ is also taken into account.

Figure 3.12 shows the spectrum of the Hamiltonian (3.59) as a function of γ at a typical deformation $\beta = 5A^{-2/3}$. On the prolate side ($\gamma = 0$) and on the oblate side ($\gamma = 60°$) we see again the same spectra as in Fig. 3.10. However, these two limits are now connected through a circle in the β, γ plane (Fig. 1.4) with constant deformation β. We no longer pass through the weak coupling limit at $\beta = 0$. On both sides the spectra do not depend very drastically on the triaxiality γ. The essential transition from the strongly coupled to the decoupled scheme takes place in a relatively small γ region around $\gamma = 30°$. There are many spectra in weakly deformed transitional nuclei that can be nicely reproduced with γ-values between 20° and 40°. This agreement can be improved even more by incorporating the change of the moment of inertia in a VMI-model type calculation [FT 75].

* Recently, Bengtsson et al. [BHM 78] have found an oscillating behavior of this interaction as a function of the chemical potential λ. For an interpretation of this fact see [FPS 80] and the references given there.

† For extension of the triaxial rotor model to multiparticle configurations, see [TNV 77, YTF 77, TYF 77, YTF 78].